A&A 457, 623–627 (2006)
DOI: 10.1051/0004-6361:20065491

Astronomy & Astrophysics

XMM-Newton observations of AM CVn binaries: V396 Hya and SDSS J1240–01

G. Ramsay[1], P. J. Groot[2], T. Marsh[3], G. Nelemans[2], D. Steeghs[4], and P. Hakala[5,6]

[1] Mullard Space Science Laboratory, University College London, Holmbury St Mary, Dorking, Surrey RH5 6NT, UK
e-mail: gtbr@mssl.ucl.ac.uk
[2] Department of Astrophysics, IMAPP, Radboud University of Nijmegen, PO Box 9010, 6500 Nijmegen, The Netherlands
[3] Department of Physics, University of Warwick, Coventry CV4 7AL, UK
[4] Harvard-Smithsonian Center for Astrophysics, 60 Garden Street, MS-67, Cambridge, MA 02138, USA
[5] Observatory, PO Box 14, 00014 University of Helsinki, Finland
[6] Tuorla Observatory, Väisäläntie 20, 21500 Piikkiö, Finland

Received 25 April 2006 / Accepted 1 July 2006

ABSTRACT

We present the results of *XMM-Newton* observations of two AM CVn systems – V396 Hya and SDSS J1240-01. Both systems are detected in X-rays and in the UV: neither shows coherent variability in their light curves. We compare the rms variability of the X-ray and UV power spectra of these sources with other AM CVn systems. Apart from ES Cet, AM CVn sources are not strongly variable in X-rays, while in the UV the degree of variability is related to the systems apparent brightness. The X-ray spectra of V396 Hya and SDSS J1240-01 show highly non-solar abundances, requiring enhanced nitrogen to obtain good fits. We compare the UV and X-ray luminosities for 7 AM CVn systems using recent distances. We find that the X-ray luminosity is not strongly dependent upon orbital period. However, the UV luminosity is highly correlated with orbital period with the UV luminosity decreasing with increasing orbital period. We expect that this is due to the accretion disk making an increasingly strong contribution to the UV emission at shorter periods. The implied luminosities are in remarkably good agreement with predictions.

Key words. accretion, accretion disks – stars: binaries: close – stars: novae, cataclysmic variables – stars: white dwarfs – X-rays: binaries – ultraviolet: stars

1. Introduction

Ultra-compact AM CVn binaries consist of a white dwarf which accretes from a degenerate (or semi-degenerate) companion star in a very short period binary. They are observed to have orbital periods shorter than ∼70 min. These systems allow us to observe accretion flows which are hydrogen-deficient, which provides an important comparison with their hydrogen-dominated counterparts (the "classical" cataclysmic variables).

Until very recently they were not well studied in X-rays or in the UV. Ramsay et al. (2005) presented *XMM-Newton* observations of 4 AM CVn system which showed that each system was easily detected at X-ray energies. Further, they showed that a large proportion of the accretion energy of AM CVn systems was emitted in the UV. Observations of the shortest period AM CVn, ES Cet, shows that it too is seen in X-rays (Strohmayer 2004b). (The two systems with shorter periods, RX J0806+15 at 5.3 min and RX J1914+24 at 9.5 min remain candidate AM CVn systems.)

Until now, the sample of AM CVn systems which have been observed using dedicated X-rays observations has been biased towards shorter orbital periods. To rectify this bias we have obtained observations of two AM CVn systems which have relatively long orbital periods. V396 Hya (also known as CE 315, Ruiz et al. 2001a), with a period of 65.2 min has the longest orbital period of known AM CVn systems, while SDSS J124058.03-015919.2 (hereafter SDSS J1240-01, Roelofs et al. 2004, 2005) has the third longest (37.4 min).

2. Observations

XMM-Newton has 3 broad-band X-ray detectors with medium energy resolution and also a 30 cm optical/UV telescope (the Optical Monitor, OM: Mason et al. 2001). The X-ray instruments contain imaging detectors covering the energy range 0.15−10 keV; one EPIC pn detector (Strüder et al. 2001) and two EPIC MOS detectors (Turner et al. 2001). Two high resolution grating spectrometers (the RGS) are also on board, but our sources are too faint to obtain useful spectra. The observation log is shown in Table 1 where we show the mean X-ray and UV count rates for each source.

The data were processed using the *XMM-Newton Science Analysis Software* (SAS) v6.5 and analysed in a similar manner to that described in Ramsay et al. (2005). For the OM observations, we used the UVW1 filter which has a central wavelength of 2910 Å and a range of 2400−3400 Å. In the case of V396 Hya, the source was just outside the fast window mode which has a small field of view (V396 Hya also has a significant proper motion, Ruiz et al. 2001b). It was, however, seen in full window mode which gives the mean brightness over a time interval of typically 4400 s. In contrast SDSS J1240-01 was observed in the OM fast window mode.

3. Light curves

V396 Hya was relatively bright in X-rays (Table 1) giving an apparent count rate greater than that of AM CVn and CR Boo, but less than HP Lib and GP Com (Ramsay et al. 2005). In contrast

Table 1. The observation log for V396 Hya and SDSS J1240-01. The exposure time is that of the EPIC pn detector. The count rate refers to the mean count rate in the EPIC pn detector (0.15−10 keV) and the UVW1 filter (2400−3400 Å).

Source	Date	Exp (ks)	EPIC Ct/s	UV Ct/s
V396 Hya	2005-07-20	27.9	0.38	1.65
SDSS J1240-01	2006-01-07	22.2	0.023	0.44

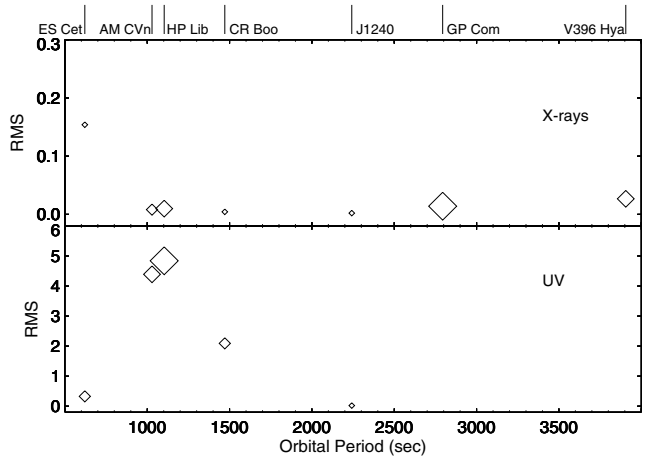

Fig. 1. The rms of the amplitude spectra of the light curves of AM CVn systems in the 0.1−1.0 keV X-ray band (*top panel*) and the UV (*bottom panel*). The size of the symbol reflects the apparent brightness in that energy. No UV fast mode data were obtained of GP Com and V396 Hya.

SDSS J1240-01 is fainter than all of the above, and only slightly brighter than ES Cet (Steeghs et al. 2006). There is evidence for some structure in the X-ray light curve of V396 Hya, but little in SDSS J1240-01. In the UV, both sources were relatively bright, but fainter than the AM CVn sources reported by Ramsay et al. (2005) and also ES Cet (Steeghs et al. 2006). We searched for periodic variations in the X-ray and UV light curves of V396 Hya and SDSS J1240-01, but found none.

To determine the level of variability for our wider sample of AM CVn systems, we measured the rms of the power spectra for each of the X-ray and UV light curves. We did this for the 0.15−1 keV energy band and the *UVW1* filter using light curves with 10 s time bins. The results are shown in Fig. 1 where the size of the symbol reflects the relative brightness in X-rays and the UV. In the X-ray band, there is no evidence for a correlation between the degree of variability and orbital period apart from ES Cet, which has the shortest orbital period and shows the largest rms. In the UV, the degree of variability appears to be related to the apparent brightness of the system, with the rms increasing with increasing brightness.

Our variability measure reflects continuum variability at only one epoch. For instance GP Com showed large variations in its UV line emission which was taken to be due to irradiation of the accretion disk or variable mass loss in a wind (Marsh et al. 1995). Further, van Teeseling & Verbunt (1994) showed a significant variation in the soft X-ray light curve of GP Com in *ROSAT* observations.

4. Spectra

The X-ray spectra of the AM CVn systems in our earlier sample were best fitted using a relatively low temperature thermal plasma model with non-solar metallicities (e.g. Strohmayer 2004a; Ramsay et al. 2005). UV Observations of V396 Hya made using the *HST* also show a significant enhancement of nitrogen (Gänsicke et al. 2003). We extracted spectra in the same manner as before, but filtered out time intervals of enhanced background. We fitted the spectra using the `cevmkl` model in `XSPEC` together with a neutral absorption model. The fits to the spectra using abundances expected from relatively low temperature CNO processed material were poor: for the EPIC pn spectra the fits were $\chi^2_\nu = 3.52$ (173 d.o.f.) for V396 Hya and $\chi^2_\nu = 2.44$ (12 d.o.f.) for SDSS J1240-01.

We then set the abundances of each element to zero (i.e. a completely ionised plasma) and then allowed each element to vary. If there was no significant improvement to the fit, then the abundance of that element was set back to zero and frozen. For both V396 Hya and SDSS J1240-01 we find that a significant amount of N improved the fits, while in the case of V396 Hya a significant amount of Ne and less significant amount of Ca also improved the fits. Fits using the EPIC MOS data were in agreement with these findings. The EPIC pn spectra of each source together with their best fits are shown in Fig. 2 while the best fit spectral parameters are shown in Table 2.

To test the robustness of these results we also fitted the X-ray spectra assuming solar abundances apart from hydrogen which was set to zero. Each element was then allowed to vary in abundance: if this resulted in no significant difference to the fit, it was re-fixed to the solar value. In the case of SDSS J1240-01 we find that nitrogen with an abundance of 55% greater than solar gave a better fit to the spectrum (at the 99.1% confidence level) and in the case of V396 Hya at an amount of 68−92% greater than solar (at >99.99% confidence). Other spectral parameters, such as the amount of absorption and the maximum temperature of the plasma, were similar to that found before (cf. Table 2). In this test, we found no evidence for an enhancement of neon in the X-ray spectrum of V396 Hya. We conclude that nitrogen is significantly enhanced in the X-ray spectra of V396 Hya and SDSS J1240-01.

5. The X-ray/UV colours of AM CVn systems

Ramsay et al. (2005) showed that AM CVn, HP Lib and CR Boo showed a much lower soft X-ray to UV ratio compared to most hydrogen accreting Cataclysmic Variables (CVs). In contrast, GP Com showed a ratio similar to that of the hydrogen accreting CVs. We are now able to increase this sample by including SDSS J1240-01, V396 Hya and ES Cet (Steeghs et al. 2006).

We adopt the same procedure as Ramsay et al. (2005). We determined the unabsorbed fluxes by setting the absorption parameter in the model fits discussed earlier to zero and calculated the unabsorbed fluxes in the 0.15−0.5 keV, 2−10 keV and *UVW1* filter pass bands. These fluxes were converted to erg s^{-1} cm^{-2} $Å^{-1}$ and their colours in the 0.1−0.5 keV/UV, 0.15−0.5/2−10 keV plane are shown in Fig. 3.

It is noticeable that systems with orbital periods shorter than 25 min are concentrated in the lower left hand corner of the colour−colour plane, ie compared to other CVs they show either a low soft X-ray flux or a high UV flux. In contrast, systems with orbital periods longer than 25 min, show a steadily increasing soft X-ray/UV ratio. We also show the position of the candidate system RX J0806+15, which is located in the far top right hand corner of the colour−colour plane. This is not unexpected since there is evidence that this system could be powered by a non-accretion mechanism and so therefore would be expected to show different X-ray/UV colours (e.g. Hakala et al. 2004).

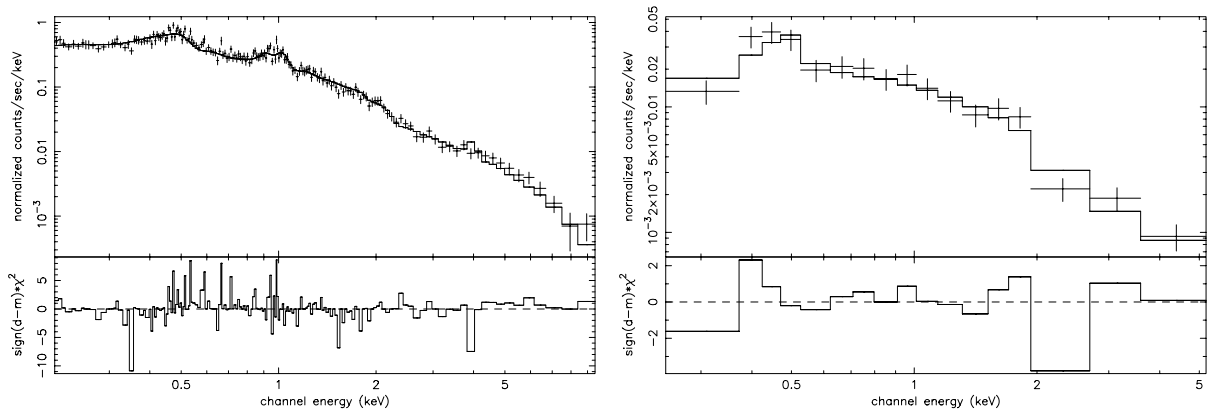

Fig. 2. The EPIC pn spectra for V396 Hya (*left panel*) and SDSS J1240-01 (*right panel*) together with the best model fits using an absorbed thermal plasma model with variable metal abundances.

Table 2. The spectral parameters derived from fitting an absorbed multi-temperature thermal plasma model with variable metal abundance, Z, to the *XMM-Newton* EPIC pn data. The slope of the power law distribution of temperature, α, was fixed at 0.5, and the maximum temperature, $T_{\rm max}$ of the plasma are shown. We initially set all the elements to zero and allowed the abundance of each individual element to vary. We show the observed X-ray flux in the 0.15−10 keV band, $F_{\rm x,o}$, the unabsorbed, bolometric X-ray flux, $F_{{\rm x},u}$, the bolometric X-ray luminosity, $L_{\rm X}$. In determining the luminosities we assume a distance of 76 pc for V396 Hya and 400 pc for SDSS J1240-01 (Table 3).

Source	$N_{\rm H}$ $\times 10^{20}$ cm^{-2}	$T_{\rm max}$ (keV)	Z (solar)	$F_{\rm x,o}$ erg s^{-1} cm^{-2}	$F_{{\rm x},u}$ erg s^{-1} cm^{-2}	$L_{\rm X}$ erg/s	χ^2_ν(d.o.f.)
V396 Hya	$3.4^{+0.9}_{-0.6}$	$5.5^{+0.5}_{-0.7}$	6 ± 1.2 (N) 0.8 ± 0.2 (Ne)	$1.05^{+0.11}_{-0.07} \times 10^{-12}$	$2.42^{+0.24}_{-0.16} \times 10^{-12}$	$1.7^{+0.2}_{-0.1} \times 10^{30}$	1.30 (170)
SDSS J1240-01	$9.0^{+7}_{-0.5}$	$6.1^{+8.3}_{-3.2}$	$7.2^{+8.7}_{-5.1}$ (N)	$9.0^{+4.5}_{-3.2} \times 10^{-14}$	$1.7^{+0.8}_{-0.6} \times 10^{-13}$	$8.2^{+2.8}_{-2.1} \times 10^{30}$	1.19 (12)

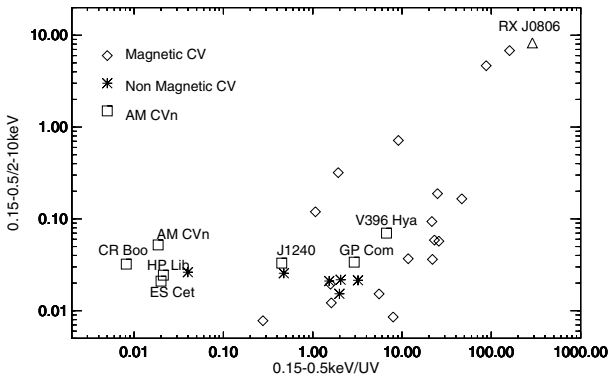

Fig. 3. The colours for the AM CVn systems in this paper; non-magnetic CVs and the strongly magnetic CVs in the 0.15−0.5/2−10 keV, 0.15−0.5/UV plane. We also show the colours of the candidate system RX J0806+15. The error on the colours are of a similar size as the symbols.

It is predicted that for systems with shorter orbital periods the emission from an accretion disk will dominate the UV emission while for longer orbital periods the white dwarf will dominate (e.g. Bildsten et al. 2006). This would naturally result in the observed trend in the AM CVn colours seen in Fig. 3. To test this we determine the X-ray and UV luminosities in the next section: the UV luminosity should increase with decreasing orbital period.

6. Luminosities

Since the paper of Ramsay et al. (2005) was published a more accurate distance has been obtained for AM CVn and distances have been obtained for the other systems included in this survey. We therefore determine the X-ray and UV luminosities for our sample using the latest distances (tabulated in Table 3). We note that the quoted distance to ES Cet was determined using the relationship between M_V and the equivalent width of the He I λ 5876 Å line and therefore is rather uncertain (Espaillat et al. 2005). The same authors note it could be as high as 1 kpc.

The unabsorbed, bolometric, X-ray luminosity was determined using the model fits to the X-ray spectra shown in Ramsay et al. (2005) and in Table 2. We assume the X-ray emission is isotropic. Since we generally have only one UV photometric point from the *XMM-Newton* OM, determining the UV luminosity is therefore more model dependent than the X-ray luminosity. We assume a blackbody of given temperature then scale the normalisation to match the observed flux at the peak of the *UVW1* filter passband (2910 Å). Although this method is rather crude, a comparison between the above method and the flux determined using the *IUE* spectrum of AM CVn we found that luminosities were consistent to within 50%.

A second consideration is correctly modelling the absorption component. Since the neutral absorption models in the X-ray spectral fitting package XSPEC (Arnaud 1996) are not applicable at UV wavelengths, we also included the `UVRED` model and tied this to the hydrogen column density parameter using the relationship between optical extinction and total absorption column of Bohlin et al. (1978).

We also note that UV emission is likely to be due to a combination of the heated white dwarf, the accretion stream and accretion disc. While it is predicted that the disc/stream component will be greater for shorter periods, taking a mean temperature to represent the UV emission is clearly somewhat simplistic. However, observations of CP Eri showed a temperature

Table 3. The distances to our sample of AM CVn systems. The distance to ES Cet is not certain.

Source	Distance (pc)	Reference
ES Cet	350	Espaillat et al. (2005)
AM CVn	606^{+135}_{-95}	Roelofs et al. (2006)
HP Lib	197^{+13}_{-12}	Roelofs et al. (2006)
CR Boo	337^{+43}_{-35}	Roelofs et al. (2006)
J1240-01	350−440	Roelofs et al. (2005)
	525	Bildsten et al. (2006)
GP Com	75 ± 2	Roelofs et al. (2006)
V396 Hya	76^{+11}_{-8}	Thorstensen (priv. com.)

Table 4. The X-ray and UV luminosities of our sample of AM CVn systems. We estimate the UV luminosities are accurate to within a factor of ∼2−4 (see Sect. 6). We assume a distance of 500 pc for RX J0806+15, 1 kpc for ES Cet and 400 pc for SDSS J1240-01.

Source	$L_{\rm UV}$ erg s^{-1}	L_X erg s^{-1}
J0806+15	4.5×10^{31}	1.5×10^{32}
ES Cet	1.4×10^{34}	8.2×10^{30}
AM CVn	1.1×10^{34}	2.8×10^{31}
HP Lib	1.0×10^{34}	1.4×10^{31}
CR Boo	2.7×10^{33}	5.2×10^{30}
J1240-01	9.2×10^{31}	8.2×10^{30}
GP Com	1.5×10^{31}	5.2×10^{30}
V396 Hya	7.5×10^{30}	1.7×10^{30}

of 17 000 K in the quiescent state (Sion et al. 2006). Further, predictions show that the effective temperature is expected to be in the range of ∼10 000−40 000 K (e.g. Bildsten et al. 2006). To determine how sensitive our derived UV luminosities were to the assumed temperature, we determined the luminosity using blackbody temperatures between 10 000−40 000 K. We find that compared to a blackbody of $kT_{\rm bb}$ = 20 000 K a blackbody of $kT_{\rm bb}$ = 10 000 K gives a luminosity a factor of 1.3 lower, while a blackbody of $kT_{\rm bb}$ = 40 000 K gives a luminosity a factor of 3.6 greater. We therefore estimate our UV luminosities will be uncertain by a factor of ∼2−4.

We show the X-ray and UV luminosities in Table 4 and in Fig. 4. Considering the X-ray luminosity, $L_{\rm X}$, as a function of orbital period, $P_{\rm orb}$, first. There is no strong relationship between $L_{\rm X}$ and $P_{\rm orb}$. We do note however, that AM CVn and HP Lib (with short $P_{\rm orb}$) have higher $L_{\rm X}$ than V396 Hya (the highest $P_{\rm orb}$). The uncertainty to the distance to ES Cet gives a correspondingly large uncertainty in its $L_{\rm X}$. In contrast, there is a strong correlation between the UV luminosity, $L_{\rm UV}$, and $P_{\rm orb}$. $L_{\rm UV}$ increases by 3 orders of magnitude over the orbital period range of AM CVn systems. This suggests that the decreasing soft X-ray/UV ratio seen for AM CVn systems in Fig. 3 is due to the UV luminosity greatly increasing for shorter binary orbital periods. The distance to RX J0806+15 is rather uncertain, but the UV luminosity does not follow the relationship for the other AM CVn systems. Indeed, in contrast to the other sources, the X-ray luminosity is greater than the UV luminosity. This is consistent with a non-accretion mechanism powering this source.

7. Discussion

7.1. Abundances

In the optical, V396 Hya and SDSS J1240-01 appear to show different abundances, with the former showing helium lines and only a small number of nitrogen lines (Ruiz et al. 2001a), while the latter also shows silicon and iron lines (Roelofs et al. 2005). V396 Hya shows an optical spectrum similar to GP Com and is thought to be a population II halo object, while SDSS J1240-01 is thought to be an "ordinary" population I object, with a higher overall metal abundance (Roelofs et al. 2005).

Our fits to the X-ray spectra of both V396 Hya and SDSS J1240-01 show a significant enhancement of nitrogen compared to both the solar abundance and the expected abundance from relatively low temperature CNO processed material. This is consistent with the fits to the X-ray spectra of AM CVn, HP Lib, CR Boo and GP Com (Ramsay et al. 2005). The apparent absence of metals other than nitrogen in the X-ray spectrum of SDSS J1240-01 could be due to the lower signal to noise of the spectrum compared to the spectrum of V396 Hya.

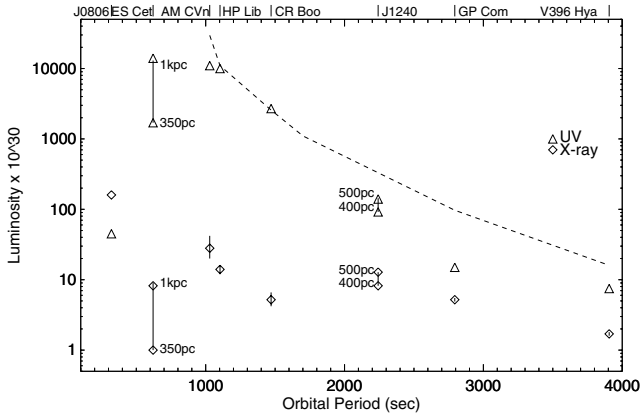

Fig. 4. The (unabsorbed) X-ray and UV luminosities of the AM CVn systems included in this sample. The X-ray luminosities were determined using modelling the X-ray spectrum derived from *XMM-Newton* data, and the UV luminosities were determined assuming a blackbody of temperature of 30 000 K. The dotted line is the predicted accretion luminosity – see Sect. 7.2 for details.

7.2. Luminosities and colours

For hydrogen accreting CVs, the orbital evolution is driven by angular momentum loss via gravitational radiation and magnetic breaking. As systems evolve to shorter orbital periods the mass transfer rate decreases by 2−3 orders of magnitude (e.g. King 1988). In the case of AM CVn binaries, angular momentum loss is driven entirely by gravitational radiation. Over the orbital period distribution of AM CVn systems, this results in a change in the mass transfer rate of 6−7 orders of magnitude, with the highest rate at short orbital periods (e.g. Nelemans et al. 2001). For both hydrogen CVs and AM CVn systems, the mass transfer rate is expected to be correlated to the accretion luminosity.

We find that in AM CVn binaries, the UV luminosity is strongly correlated with the binary orbital period, with the UV luminosity increasing as the orbital period gets shorter. The relationship is so pronounced that it is unlikely to be due to uncertainties in our method of determining the UV luminosity. This is in contrast to hydrogen accreting CVs which show the opposite relationship: $L_{\rm UV}$ decreases as the orbital period gets shorter (van Teeseling et al. 1996). This is consistent with our view of how these binaries evolve.

The strong relationship between $L_{\rm UV}$ and $P_{\rm orb}$ for AM CVn systems allows us to show that the decreasing soft X-ray/UV ratio shown in Fig. 3 is due to the increasing UV luminosity of the system. We suggest that this is due to UV emission from the

accretion disk which gets increasingly prominent for systems with orbital period less than ∼25 min. We note that based on this relationship, a "high" distance to ES Cet is favoured.

The lack of a strong relationship between the X-ray luminosity and the orbital period is also noted amongst hydrogen accreting CVs. Only a weak relationship is seen (van Teeseling et al. 1996; Baskill et al. 2005). In both hydrogen accreting systems and in AM CVn systems, it appears that the change in the accretion rate is reflected in the UV emission rather than in X-rays.

How does the predicted luminosity compare with the observed X-ray and UV luminosities? We simplify matters by assuming the accretion luminosity can be approximated by $L_{\rm acc} = GM_1\dot{M}/R$ (in reality it is expected to be more complex than this) and the mass of the primary star, M_1, is taken to be 0.6 $M_\odot$ (again in reality M_1 will span a range in mass). Again, as we noted earlier, some fraction of the UV flux will originate from the heated white dwarf. However, at longer orbital periods, where the heated white dwarf is expected to make a greater contribution to the UV flux, its luminosity is expected to be several orders of magnitude less than the solar luminosity, implying that this is a valid assumption (Bildsten et al. 2006).

We have taken the predicted mass transfer rate for different sources in Table 1 of Deloye et al. (2005). The mass transfer rate is set by a number of factors including the mass of the primary and secondary stars and the secondary stars specific entropy. We took the mean mass transfer rate for each system and smoothed the resulting curve of $\dot{M}$ as a function of $P_{\rm orb}$: this is shown in Fig. 4. The agreement with the UV luminosity, especially at shorter orbital periods in remarkable. At longer orbital periods the predicted luminosity is slightly in excess of the combined X-ray and UV luminosity, suggesting that for these long period systems, a significant fraction of the accretion luminosity is emitted at optical wavelengths.

8. Conclusions

We have presented X-ray and UV observations of AM CVn binaries which sample their full orbital period distribution. We find that there is no evidence for coherent modulations in their X-ray signal. In the UV, we find strong variability in their signal between orbital periods of ∼1000−1500 s, although there is no correlation between the degree of fractional variability and orbital period.

We find that the soft X-ray/UV ratio decreases as the system orbital period decreases. This is due to the UV luminosity increasing strongly as the orbital period decreases. We suggest that this effect is due to the accretion disc providing an increasingly dominant contribution to the UV flux as shorter periods. The observed luminosities are in remarkably good agreement with that predicted and also indicates that at longer orbital periods a significant fraction of the accretion energy is also emitted at optical wavelengths.

Our results suggest that new AM CVn systems could be discovered in X-ray/UV surveys due to their UV variability and their X-ray/UV colours.

Acknowledgements. This paper is based on observations obtained using *XMM-Newton*, an ESA science mission with instruments and contributions directly funded by ESA Member States and the USA (NASA). We thank John Thorstensen for communicating the distance of V396 Hya prior to publication. P.H. is supported by the Academy of Finland, D.S. acknowledges a Smithsonian Astrophysical Observatory Clay Fellowship and support through NASA GO grants NNG04G30G and NNG06GC05G, P.J.G. is supported by NWO VIDI grant 639.042.201, G.N. by NWO VENI grant 639.041.405 and T.R.M. was supported by a PPARC Senior Fellowship during the course of this work.

References

Arnaud, K. A. 1996, Astronomical Data Analysis Software and Systems V, ed. G. Jacoby, & J. Barnes, ASP Conf. Ser., 101, 17
Baskill, D. S., Wheatley, P. J., & Osborne, J. P. 2005, MNRAS, 357, 626
Bildsten, L., Townsley, D. M., Deloye, C. J., & Nelemans, G. 2006, ApJ, 640, 466
Bohlin, R. C., Savage, B. D., & Drake, J. F. 1978, ApJ, 224, 132
Deloye, C. J., Bildsten, L., & Nelemans, G. 2005, ApJ, 624, 934
Espaillat, C., Patterson, J., Warner, B., & Woudt, P. 2005, PASP, 117, 189
Gänsicke, B. T., Szkody, P., de Martino, D., et al. 2003, ApJ, 594, 443
Hakala, P., Ramsay, G., & Byckling, K. 2004, MNRAS, 453
King, A. R. 1988, QJRAS, 29, 1
Marsh, T. R., Wood, J. H., Horne, K., & Lambert, D. 1995, MNRAS, 274, 452
Mason, K. O., Breeveld, A., Much, R., et al. 2001, A&A, 365, L36
Nelemans, G., Portegies Zwart, S. F., Verbunt, F., & Yungelson, L. R. 2001, A&A, 368, 939
Ramsay, G., Hakala, P., Marsh, T., et al. 2005, A&A, 440, 675
Roelofs, G. H. A., Groot, P. J., Steeghs, D., & Nelemans, G. 2004, Rev. Mex. Astron. Astrofis., 20, 254
Roelofs, G. H. A., Groot, P. J., Marsh, T. R., et al. 2005, MNRAS, 361, 487
Roelofs, G. H. A, Groot, P. J., Benedict, F. G., et al. 2006, ApJ, submitted
Ruiz, M. T., Rojo, P. M., Garay, G., & Maza, J. 2001a, ApJ, 552, 679
Ruiz, M. T., Wischnjewsky, M., Rojo, P. M., & Gonzalez, L. E. 2001b, ApJS, 133, 119
Sion, E. M., Solheim, J.-K., Szkody, P., Gaensicke, B. T., & Howell, S. B. 2006, ApJ, 636, L125
Steeghs, D., et al. 2006, ApJ, submitted
Strohmayer, T. E. 2004a, ApJ, 608, L53
Strohmayer, T. E. 2004b, ApJ, 614, 358
Strüder, L., Briel, U., Dennerl, K., et al. 2001, 365, L18
van Teeseling, A., & Verbunt, F. 1994, A&A, 292, 519
van Teeseling, A., Beuermann, K., & Verbunt, F. 1996, A&A, 315, 467
Turner, M. J. L., Abbey, A., Arnaud, M., et al. 2001, A&A, 365, L27